An International Journal
computers & mathematics with applications

PERGAMON Computers and Mathematics with Applications 44 (2002) 1129–1146
www.elsevier.com/locate/camwa

Population Kinetic Models for Social Dynamics: Dependence on Structural Parameters

M. LO SCHIAVO
Department of Mathematical Models and Methods
Università "La Sapienza", Roma, Italy

(Received July 2001; accepted August 2001)

Abstract—A kinetic equation of the Boltzmann kind is adopted to approach the analysis of a population of individuals subject to social interactions. The state variable, referred to a dominant social feature such as the individual wealth, is defined on the whole real axis. Different kinds of interactions are allowed, both on a stochastic and a deterministic basis. Structural parameters are varied, and the related system sensitivity analysed.

Keywords—Generalized Boltzmann, Population models, Social sciences, Evolution equations.

1. INTRODUCTION

This paper deals with a computational analysis of the time evolution and parameter sensitivity exhibited by a class of population kinetic models for social dynamics. The mathematical structure underlying the class consists of an integrodifferential evolution equation defined for a population density function $f \geq 0$ depending on the time $t \in [0, \infty)$ and on a scalar state variable $u \in \mathbb{R}$.

The class of models considered in this paper can be regarded as a generalization and development of a model proposed by Jager and Segel [1] to describe the social behaviours of certain populations of insects, actually the bumblebee. The mathematical model shows a structure similar to the classic Boltzmann equation, i.e., an integrodifferential equation for a suitable probability density function. Indeed, it was classified in [2] as a generalized kinetic model.

Application of generalized kinetic models in applied sciences was motivated in [3]. Indeed, several developments have been studied by many authors with reference to various fields of applied sciences. Developments refer both to mass conservative equations, as well as to models which include proliferative and destructive phenomena. For instance, the model was developed, as documented in [4,5], to describe the immune competition against invasive tumour cells. A completely different field of application is the one in [6] where a similar model was proposed to describe a multilane traffic flow. Generalization to models with transition from one population to the other is extensively developed in [7], motivated by applications to mathematical immunology [4]. Paper [7] also provides a qualitative analysis of the initial value problem. Indeed, this

Partially supported by G.N.F.M. of I.N.D.A.M.
The author is very grateful to Prof. B. Firmani for interesting and helpful discussions.

0898-1221/02/$ - see front matter Typeset by AMS-TEX
PII: S0898-1221(02)00221-3

class of models generates several interesting mathematical problems, as it is documented in the review paper [8].

The present paper follows the line of the discussion in Chapter 5 of [3], and elaborates a parameter sensitivity analysis for mass conservative models in the spatially homogeneous case. Technically finite differences methods [9] are developed to adjust suitable schemes, initiated in [10], towards the structure of the models dealt with in this paper. Sensitivity analysis is worked out with special attention to the asymptotic behaviour of the solutions.

In almost all examined cases, the system behaviour proves to be satisfactorily stable under different numerical approaches and even under variations of several control parameters. On the contrary, there are some of the parameters that produce bifurcation points, and these appear to be structurally stable, in the sense that the bifurcation is not cancelled by (reasonable) modifications of the other controls.

At generic conditions, a stable time-asymptotic distribution function has been found. However, in few and extreme cases (generally in the bifurcation neighbourhoods), the numerical precision is hardly sufficient to guarantee the result in all its details, although it is possible to induce them by analysing the complete picture.

The contents are organized into three additional sections which follow this introduction. Section 2 deals with a brief description of the models, and it reports the main assumptions that have been used to frame them. Section 3 deals with the development of a suitable computational scheme that starts from finite differences method. Section 4 deals with simulations and parameter sensitivity. The analysis is followed by a brief conclusive discussion.

2. MODELS DESCRIPTION

As already mentioned in the introduction, this paper deals with a suitable development of the Jager and Segel model. It can be regarded as a population dynamics model for interacting individuals with an internal structure (identified in what follows by a scalar variable u). Interactions do not modify the number of individuals (the size of the population), but modify the state of the interacting individuals. Therefore, rather than studying the evolution of the total number of individuals as in traditional population dynamics models, see, e.g. [11], we are interested in the evolution of the interacting individuals statistical distribution over the above-mentioned internal state.

Specifically this paper refers to the modelling of human social competition; the state variable $u \in \mathbb{R}$ is meant to represent the *social state*, from low to high social level, of the individuals of the population. Negative values of u correspond to poor social state, which is extreme for $u \to -\infty$; positive values correspond to wealthy social state. The value $u = 0$ marks the separation between poverty and wealth.

The dependent variable of the evolution equation is a nonnegative function

$$f = f(t, u); \qquad f : [0, \infty) \times \mathbb{R} \to [0, \infty), \tag{2.1}$$

which is a population density, in the sense that the value

$$N(t, V) = \int_V f(t, u)\, du \tag{2.2}$$

assigns the expected number of individuals to be found at time t with states in a (regular) subset V of the phase state space. For instance, $V = [u_1, u_2] \subset \mathbb{R}$.

For the problems to be meaningful, f has to be integrable for each $t \geq 0$; that is, it will be assumed that

$$\int_{-\infty}^{\infty} f(t, u)\, du = N(t) < \infty, \qquad \text{for each } t \geq 0. \tag{2.3}$$

In fact, due to the particular structure of the evolution equation considered here, the integral in equation (2.3), which represents the *total number* of individuals in the population, is a constant

$$N(t) = N(0) =: N_0. \tag{2.4}$$

On the other hand, in order that the initial conditions may correspond to some effectively observed social distribution, a value u_0 may be introduced such that the value N_0 is assigned by

$$N(t = 0,\ u \in [-u_0, u_0]) \simeq N_0. \tag{2.5}$$

For instance, and this is what it will be done in the simulations that follow, one may assume that the initial distribution is given by

$$f(t = 0, u) =: f_0(u) \equiv N_0\, g_0(u), \tag{2.6}$$

where g_0 is a truncated normal distribution with *a priori* known mean value m_0, variance σ_0, and support $[-u_0, u_0]$,

$$g_0(u) = \begin{cases} \dfrac{1}{\sqrt{2\pi\sigma_0}} \exp -\dfrac{(u - m_0)^2}{2\sigma_0}, & \text{for } u \in [-u_0, u_0], \\ 0, & \text{otherwise.} \end{cases} \tag{2.7}$$

Here m_0, which may be either positive or negative, is meant to represent the actually observed mean value of the initial social state, and $\sigma_0 > 0$ refers on how much the observed initial population wealth is concentrated around m_0. For σ_0 small enough, u_0 may be identified with some critical value u_c such that the population $N(t = 0,\ u \in [-u_c, u_c])$ satisfactorily approximates the population value of the complete normal distribution over $\mathbb{R}$. The constancy of the total population value $N = N(t)$ allows us to renormalize the density function f to a probability density function, and interpret the integral in equation (2.2) as the probability of finding an individual at time t in a state $u \in V$.

As in the model proposed by Jager and Segel, microscopic interactions among the individuals are taken into account by introducing a pair of terms, η and ψ, respectively, modelling the rate of encounters between individuals and the transition probability density which modifies the state of each individual subject to an encounter. More in detail, a nonnegative function $\eta = \eta(v, w)$ for the *encounter rate* refers to the expected number of pairwise encounters per unit time between individuals in the state v and individuals in the state w. The transition of an individual from the state v to the state u because of an encounter with an individual in the state w admits a *transition probability density*, with respect to the variable u, denoted by $\psi(u; v, w) \geq 0$. Only binary encounters are considered. Factorization of the joint probability is assumed. Neither the encounter rate nor the transition probability density explicitly depend on the time.

In addition, it is supposed that interactions are the only possible mechanism for the individuals to change their states. Namely, it is *a priori* assumed that no external field acts on the system $\dot{u} = 0$, and hence, that the total time derivative of the distribution f identically equals its partial derivative.

The evolution equation for the density functions f is obtained, as in the Boltzmann case, by equating the time derivative of f to a balance between *gain* and *loss* terms. In particular, the mathematical structure resides in the balance equation

$$\frac{\partial f}{\partial t} = G[f] - L[f], \tag{2.8}$$

where the gain and loss terms have the following expressions:

$$G[f](t, u) = \int_{-\infty}^{\infty} \int_{-\infty}^{\infty} \eta(v, w)\psi(u; v, w) f(t, v) f(t, w)\, dv\, dw, \tag{2.9}$$

$$L[f](t, u) = f(t, u) \int_{-\infty}^{\infty} \eta(u, w) f(t, w)\, dw. \tag{2.10}$$

Starting from the above model, and in order to be more specific about the interactions between individuals, the following procedure will be adopted. First, some peculiar features are discussed that characterize the interaction procedures and different kinds of interactions are supposed to happen. Then, the occurrence of each interaction kind is assumed to be controlled either on a deterministic basis, or as a stochastic event. Finally, a further specialization is possibly introduced of the functions η, ψ, that acquire the meaning of conditional quantities, and as many of them defined as many interaction kinds are considered. In the details, let a (discrete) set $\mathbb{L} \subset \mathbb{N}$ sample the various procedures, and $\ell \in \mathbb{L}$ be the corresponding label for the interaction character. Equations (2.9) and (2.10) are written as follows:

$$G[f](t,u) = \sum_{\ell \in \mathbb{L}} \int_{-\infty}^{\infty} \int_{-\infty}^{\infty} q_\ell \eta_\ell(v,w) \psi(u;v,w;\ell) f(t,v) f(t,w)\, dv\, dw, \tag{2.9'}$$

$$L[f](t,u) = \sum_{\ell \in \mathbb{L}} f(t,u) \int_{-\infty}^{\infty} q_\ell \eta_\ell(u,w) f(t,w)\, dw, \tag{2.10'}$$

where q_ℓ denoted the probability of occurrence of the ℓ^{th} kind of interaction, and may be set equal to one in the deterministic case.

The aim of this paper is to analyse the social behaviours that happen when people of different social power, specifically of different wealth, are subject to mutual interactions. Correspondingly, a sampling may be tuned according to the desire and friendship that the individuals feel in encountering and interacting with each other, and possibly to the degree of individual profit or social balance that is produced by the interaction. Admittedly, these features influence not only the actual occurrence of each kind of interaction, but also the (conditional) frequencies and expected output states.

As the frequency η is concerned, specialization may yield different functions of the individual states. For instance, people with very different social states may be hindered in undergoing balanced business-like interactions and only suffer disruptive connections. On the contrary, similar social states act in favour of cooperative exchanges or, at least, more easily allow an even redistribution of the resources.

Even stronger is the effect that the different interaction characters may induce not only on the specific values of the transition probability density ψ, but even on its qualitative shape altogether. In this paper, the following details will be adopted. The transition function ψ is a probability density with respect to its first variable, i.e.,

$$\int_{-\infty}^{+\infty} \psi(u;v,w;\ell)\, du = 1, \qquad \text{for each } v,w \in \mathbb{R},\ \ell \in \mathbb{L}. \tag{2.11}$$

Regarding the dependence of ψ on the other state variables, the same simple idea is used here as it was done for the initial distribution function; namely, the function ψ is selected from the family of probability densities on $\mathbb{R}$ that are completely characterized by assigning their first and second moments, i.e., the mean value m and variance σ of the random variable they depend upon. Specifically, it is assumed that the *mean value* m of the post interaction state u (of the incoming individual who leaves the state v), and its *standard deviation* σ, are *a priori* known per each value of ℓ, v, and w; and that this knowledge is sufficient to assign the value of the function ψ at each point u. Namely, both m and σ are given as functions of the state variables of the incoming individuals per each interaction procedure,

$$\begin{aligned} &m = m_\ell(v,w) \in \mathbb{R}; \\ &\sigma = \sigma_\ell(v,w) > 0; \end{aligned} \qquad u,v \in \mathbb{R}, \quad \ell \in \mathbb{L}. \tag{2.12}$$

Consequently, function ψ may be written as

$$\psi(u;v,w;\ell) = \psi\left(u; m_\ell(v,w), \sigma_\ell(v,w)\right), \tag{2.13}$$

provided that

$$m = \int_{-\infty}^{+\infty} u\,\psi(u, m, \sigma)\,du; \qquad \sigma = \int_{-\infty}^{+\infty} (u-m)^2 \psi(u; m, \sigma)\,du. \tag{2.14}$$

The qualitative shape of the function ψ being *a priori* fixed, the various interaction characters affect only the values of m and σ. For instance, an interaction with the character of social assistance, or at least with protective social rules, preludes to a mean value m which is inside the interval $(v-w)$: this interaction is of *altruistic nature*. Conversely, when the logic of a strict individual profit implies that the state of the incoming individual is enhanced in the expected output state, then the interaction is of *competitive nature*.

With these assumptions, equations (2.9′) and (2.10′) acquire their final form

$$G[f](t,u) = \sum_{\ell \in \mathbb{L}} \int_{-\infty}^{\infty} \int_{-\infty}^{\infty} q_\ell\, \eta_\ell(v,w) \psi(u; m_\ell(v,w), \sigma_\ell(v,w)) f(t,v) f(t,w)\,dv\,dw, \tag{2.9″}$$

$$L[f](t,u) = \sum_{\ell \in \mathbb{L}} f(t,u) \int_{-\infty}^{\infty} q_\ell\, \eta_\ell(u,w) f(t,w)\,dw, \tag{2.10″}$$

which may hold both in the deterministic and the stochastic approach. In the stochastic case, the set of numbers $\{q_\ell\}_{\ell \in \mathbb{L}}$ has the characters of a probability distribution

$$0 \le q_\ell \le 1, \qquad \sum_{\ell \in \mathbb{L}} q_\ell = 1, \tag{2.15}$$

and the encounter rates $\{\eta_\ell\}_{\ell \in \mathbb{L}}$ are arbitrary nonnegative integrable functions. In the deterministic case, all the numbers q_ℓ may conventionally be set to one. For the rate function η, and because of the specific form of equations (2.9′) and (2.10′), variables are redefined such as to allow the specific form

$$\eta_\ell(v,w) = \eta^0 \phi_\ell(v,w), \qquad \ell \in \mathbb{L}, \tag{2.16}$$

where $\eta^0 > 0$ is a real constant and ϕ_ℓ are such that

$$\sum_{\ell \in \mathbb{L}} \phi_\ell(v,w) = 1, \qquad v, w \in \mathbb{R}. \tag{2.17}$$

Again it has to be remarked that this picture shows two notable differences with respect to the Jager and Segel model. Specifically, u is defined over the whole real line, and more than one interaction procedures are here allowed to happen.

Within the above framework, the following assumptions appear to be appropriate to construct specific models.

ASSUMPTION 1. *The sample space $\mathbb{L}$ of the interaction characters is restricted to a binary set $\mathbb{L} := \{1, 2\}$.*

ASSUMPTION 2. *Interactions of the first kind, $\ell = 1$, denote an altruistic nature, and provide an expected mean value m inside the social states interval $(v-w)$ of the two interacting individuals. Interactions of the second kind, $\ell = 2$, denote a competitive nature. They provide, for the individual that has v as initial state, an expected mean value m that is higher than v if v is higher than w, whereas m is lower than v if v is lower than w.*

ASSUMPTION 3. *The transition probability variance σ is independent both of the interaction characters and of the social states.*

It is now possible to explicitly trace the details of the following experiments, with the aim of analysing the system behaviour at infinity, and possibly interpreting its sensitivity upon both the structural parameters and the initial conditions.

EXPERIMENT n.1. The altruistic and competitive events, respectively, have probabilities $q \geq 0$ and $1-q$. All the interactions rates are independent of the individuals' social states. The expected mean value is assigned by an easy linear law

$$m_\ell(v,w) = \begin{cases} v - \alpha(v-w), & \text{if } \ell = 1, \quad \alpha \geq 0, \\ v + \beta(v-w), & \text{if } \ell = 2, \quad \beta \geq 0. \end{cases} \tag{2.18}$$

Two shapes are adopted for the transition probability density: one localized in the immediate neighbourhood of m, the other spread all over the real axis. Specifically, the following functions are considered.

MOVABLE SQUARED DISTRIBUTION.

$$\psi_0(u;m,\sigma) = \begin{cases} (2c_s\sqrt{\sigma})^{-1}, & \text{if } u \in [m - c_s\sqrt{\sigma},\ m + c_s\sqrt{\sigma}], \\ 0, & \text{otherwise;} \quad c_s > 0. \end{cases} \tag{2.19}$$

NORMAL DISTRIBUTION.

$$\psi_3(u;m,\sigma) = \frac{1}{\sqrt{2\pi\sigma}} \exp -\frac{(u-m)^2}{2\sigma}. \tag{2.20}$$

Admittedly, no *a priori* reason really justifies this particular choice, and other well-known distributions could have been preferred, such as the following.

MOVABLE BETA DISTRIBUTION.

$$\psi_1(u;m,\sigma) = \begin{cases} \dfrac{\Gamma(r+s)}{\Gamma(r)\Gamma(s)} \left(\dfrac{u-m+c_b\sqrt{\sigma}}{2c_b\sqrt{\sigma}}\right)^{r-1} \left(\dfrac{m+c_b\sqrt{\sigma}-u}{2c_b\sqrt{\sigma}}\right)^{s-1} \dfrac{1}{2c_b\sqrt{\sigma}}, \\ \qquad \text{if } u \in [m - c_b\sqrt{\sigma},\ m + c_b\sqrt{\sigma}], \\ 0, \quad \text{otherwise;} \quad c_b > 1. \end{cases} \tag{2.21}$$

MOVABLE GAMMA DISTRIBUTION.

$$\psi_2(u;m,\sigma) = \begin{cases} \dfrac{r^s}{\Gamma(s)} (u - m + c_g\sqrt{\sigma})^{s-1} \exp\left(-r\,(u - m + c_g\sqrt{\sigma})\right) \\ \qquad \text{if } u \geq m - c_g\sqrt{\sigma}, \\ 0, \quad \text{otherwise;} \quad c_g > 0. \end{cases} \tag{2.22}$$

However, several simulations have been performed using these last two functions, and no significative differences or particular dynamics have been observed associated with either of them. Indeed, both behave quite closely to ψ_3 when c_b and c_g are greater than 3, and show some more resemblance to ψ_0 when the two constants are equal to 2. Values lower than 2 have not been pursued to avoid local spikes, which in any case do not change the overall dynamics. Hence, in what follows, reference will be made only to either ψ_0 or ψ_3.

In the next experiments, interest resides in the dependence of interaction frequency from social states rather than on the aleatory occurrence of the possible interactions. Therefore, the various kinds of interactions will be assumed to happen on a deterministic basis and, on the contrary, the conditional interaction frequencies will explicitly depend on the social states of interacting individuals. In particular, the following experiments are defined.

EXPERIMENT n.2. The altruistic and competitive events happen on a deterministic basis: $q_1 = q_2 = 1$. The interaction rates are assigned by equations (2.16) and (2.17) where the function $\phi_1 =: \phi$ is given by

$$\phi(v,w) = \frac{1}{1 + c_e\,(v-w)^2}, \qquad c_e > 0. \tag{2.23}$$

With regard to the transition probability density, all the details characterizing Experiment n.1 hold in the present one as well.

EXPERIMENT n.3. With regard to the occurrence of the interactions and to the transition probability density, all the details characterizing Experiment n.2 hold for the present one. The interaction rates of this experiment are again assigned by equations (2.16) and (2.17) where the function $\phi_1 =: \phi$ is given by

$$\phi(v,w) = \begin{cases} 1, & \text{if } |v-w| \le c_d, \\ 0, & \text{otherwise.} \end{cases} \tag{2.24}$$

However, in the numerical treatment of the model, some technical details force the introduction of slight though necessary modifications of the said functions, as it is described in the next section.

3. DISCRETIZATION SCHEME

In the preceding section, the model structure has been described without reference to the actual computations performed to generate the simulations and their results. This section is devoted to briefly summarize few technical details concerning the adopted discretization technique, and the consequent approximation procedure.

The unboundedness of phase space $\mathbb{R}$ has been represented by introducing a nonlinear function ξ mapping a prefixed interval $[A,B]$ into $[A^*,B^*] := [\xi(A),\xi(B)]$ meant to represent the real axis

$$\begin{gathered} \xi : x \in [A,B] \mapsto v = \xi(x) \in \mathbb{R}, \\ -A = B, \qquad -\xi(-x) = \xi(x), \qquad B^* = \xi(B) \gg B. \end{gathered} \tag{3.1}$$

Using this function, and defining a regular mesh for the variable x on the interval $[A,B]$, a corresponding mesh for the actual variables $u,v,w \in \mathbb{R}$ is easily obtained by the algorithm

$$\text{select} \quad \nu \in \mathbb{N}, \text{ and for } n = 1,\dots,2\nu+1,$$

$$\text{define} \quad x_n := A + (n-1)\Delta x, \text{ where } \Delta x := \frac{(B-A)}{2\nu}; \tag{3.2}$$

$$\text{then let} \quad v_n \in [A^*,B^*] \text{ be defined by } v_n := \xi(x_n). \tag{3.3}$$

In what follows, the node number is odd and written as $2\nu+1$, the central value $\nu+1$ reserved for $u = 0$, the value $-A^* = B^*$ meant to represent infinity is summarized by the parameter $\lambda := \log_{10} B^*$, and the function ξ used in most of the simulations is

$$\xi(x) = \begin{cases} -\exp\left(-\dfrac{a\,x}{100}\right) + 1, & \text{if } 100 \le x < 0, \\ \exp\left(\dfrac{a\,x}{100}\right) - 1, & \text{if } 0 \le x \le 100, \end{cases} \tag{3.4}$$

where $a = \ln(B^*+1)$.

With this method, however, a compact image of the real line is produced, that implies some minor adjustments and corrections to the above-cited functions η and ψ.

For instance, the mean value function that has been effectively employed is the following one:

$$m_\ell(v,w) = \begin{cases} v - \alpha(v-w), & \text{if } \ell = 1, \quad \alpha \ge 0, \\ v + \beta(v-w)M(v,w), & \text{if } \ell = 2, \quad \beta \ge 0, \end{cases} \tag{3.5}$$

where $M \approx 1$ for almost all values of v and w, except those that would project m_2 outside the closed numerical image: $[A^*,B^*]$ of the set $\mathbb{R}$. In particular,

$$M(v,w) = \begin{cases} 1 - \dfrac{v}{A^*}, & \text{if } v < w \text{ and } v < 0, \\ 1 - \dfrac{v}{B^*}, & \text{if } v > w \text{ and } v > 0, \\ 1, & \text{otherwise.} \end{cases} \tag{3.6}$$

Analogous truncating procedures have been adopted, when necessary, on the endings of the function ψ domain, and on the value $\hat{\sigma}$ of the transition probability density variance, especially when the mean value m approaches extreme values.

The actual discretization of the problem that corresponds to each of the experiments cited above has been accomplished as follows. A first-order scheme in time has been introduced, which specializes equation (2.8) into the following problems, for ($j = 0, 1, 2, 3$, and) $f_k(u) := f(t = t_k, u)$, $k = 0, 1, \ldots$:

$$\frac{f_{k+1}(u) - f_k(u)}{\Delta t_k} = \sum_{\ell=1}^{2} \int_{-\infty}^{+\infty} \int_{-\infty}^{+\infty} q_\ell \, \phi_\ell(v, w) \, \psi_j(u; v, w; \ell) \, f_k(v) f_k(w) \, dv \, dw - f_k(u) \int_{-\infty}^{+\infty} f_k(w) \, dw, \tag{3.7}$$

where $\{t_0 = 0, t_1, t_2, t_3, \ldots\}$ is the time discretization, and $\Delta t_k := t_{k+1} - t_k$.

Then, integration has been valued by means of an easy trapezoidal rule

$$\begin{aligned} \Delta_n &:= \frac{(v_{n+1} - v_{n-1})}{2}, \qquad \text{for } n = 2, 3, \ldots, 2\nu, \\ \Delta_1 &:= \frac{(v_2 - v_1)}{2}, \qquad \Delta_{2\nu+1} := \frac{(v_{2\nu+1} - v_{2\nu})}{2}, \end{aligned} \tag{3.8}$$

which transforms (the j^{th} of) equation (3.7) into the following set of $(2\nu + 1)$ recursive equations:

$$\frac{f_{k+1}^h - f_k^h}{\Delta t_k} = G_k^h(j) - L_k^h, \qquad h = 1, \ldots, 2\nu + 1, \tag{3.9}$$

where

$$G_k^h(j) = \sum_{\ell=1}^{2} \sum_{i=1}^{2\nu+1} \sum_{n=1}^{2\nu+1} q_\ell \, \phi_\ell^{i,n} \, \psi_j^{h,i,n}(\ell) \, f_k^i \, f_k^n \, \Delta_i \, \Delta_n, \tag{3.10}$$

$$L_k^h = f_k^h \sum_{n=1}^{2\nu+1} f_k^n \, \Delta_n, \tag{3.11}$$

and where

$$\begin{aligned} f_k^h &:= f_k(v_h), \quad \eta_\ell^{i,n} := \eta_\ell(v_i, v_n), \\ h, i, n &\in \{1, \ldots, 2\nu + 1\}, \qquad j = 0, \ldots, 3, \end{aligned} \tag{3.12}$$

and coefficients ψ will be taken from the cited functions (2.19)–(2.22) such that normalization (2.11) holds true.

On one hand, because of their assumed time independence, weights ψ may be computed once and for all at the beginning of the time series. On the other, to be ensured that for each $k = 1, 2, \ldots$ the conditions

$$\sum_{n=1}^{2\nu+1} f_k^n \, \Delta_n = N_0 \tag{3.13}$$

are satisfied with all the required accuracy, a fact that it is implicit in the structure of equations (2.8), (2.9″), (2.10″), a further renormalization of weights ψ has to be adopted. In this way, it is possible to account not only for the nodes rarefaction, that in all cases happens towards infinity, but also for the domain truncation and variance redefinition, that are needed when an *a priori* mean value m_ℓ too close to the points A^* or B^* projects either of the ψ domain endings outside the image $[A^*, B^*]$ of the real line.

To be precise, for $i,n \in \{1,\dots,2\nu+1\}$ and $\ell \in \{1,2\}$, call $\tilde{m}_\ell^{i,n}$ the *a priori* mean values assigned by equation (2.18), that is

$$\tilde{m}_\ell^{i,n} = m_\ell(v = v_i,\, w = w_n) \tag{3.14}$$

where v_i and w_n are defined by equation (3.3). Then use equations (2.19)–(2.22) to define

$$\tilde{\psi}_j^{h,i,n}(\ell) := \psi_j\left(u = u_h\colon\, \tilde{m}_\ell^{i,n},\, \hat{\sigma}\right), \tag{3.15}$$

where $\hat{\sigma} > 0$ is a constant, $h = 1,\dots,2\nu+1$, and $j = 0,\dots,3$.

Due to the facts that m_ℓ and u may be wide apart from one another, and that for any reasonable choice of $\hat{\sigma}$ there are many nodes $\{h_1, h_2, \dots\}$ such that $\sqrt{\hat{\sigma}} < \Delta_{\tilde{h}}$ for $\tilde{h} \in \{h_1, h_2, \dots\}$, it often happens that the numeric integral

$$S_j := S_j^{i,n}(\ell) := \sum_{h=1}^{2\nu+1} \tilde{\psi}_j^{h,i,n}(\ell)\,\Delta_h \tag{3.16}$$

not only is less than one, but even unreasonably small. To overcome this problem, weights $\psi_j^{h,i,n}(\ell)$ to be used in equation (3.9) have been defined as follows:

$$\psi_j^{h,i,n}(\ell) = \begin{cases} \dfrac{\tilde{\psi}_j^{h,i,n}(\ell)}{S_j^{i,n}(\ell)}, & \text{if } S \geq \tilde{S}, \\ \psi_0^{h,i,n}(\ell), & \text{if } 0 \leq S < \tilde{S}, \end{cases} \tag{3.17}$$

where $\tilde{\psi}$ is given by equation (3.15), where $\tilde{S} := 10^{-30}$, and where ψ_0 is now to be specified on account of equation (2.19).

Define

$$m_\pm = \tilde{m}_\ell^{i,n} \pm \sqrt{\hat{\sigma}} \tag{3.18}$$

and introduce the first neighbourhood nodes $\bar{h}_- \geq 1$, and $\bar{h}_+ \leq 2\nu+1$, respectively, on the left and on the right sides of the open interval (m_-, m_+), i.e., such that

$$v_h \leq m_- \text{ when } h \leq \bar{h}_-, \qquad \text{and} \qquad v_h \geq m_+ \text{ when } h \geq \bar{h}_+.$$

In this way, the interval $\bar{I}_{m,\sigma} := [v_{\bar{h}_-}, v_{\bar{h}_+}]$ is the smallest closed interval, with node endings, that contains $[m_-, m_+]$.

A first possible discretization of equation (2.19) is as follows, and in the next section this rule will be addressed to as the "AND" rule:

$$\bar{\psi}_0^{h,i,n}(\ell) = \begin{cases} \left(\Delta_h\left(\bar{h}_+ - \bar{h}_- + 1\right)\right)^{-1}, & \text{if } \bar{h}_- \leq h \leq \bar{h}_+, \\ 0, & \text{otherwise.} \end{cases} \tag{3.19}$$

Although straightforward, this definition is to be regarded as too rough, especially when the system evolution is structurally unstable. A second, tighter though questionable, discretization is obtained by excluding the nodes that lie too far from the interval $[m_-, m_+]$. That is, instead of $\bar{h}_\pm$, the following are introduced:

$$h_- := \begin{cases} \bar{h}_- + 1, & \text{if } \dfrac{\left(v_{\bar{h}_-} + v_{\bar{h}_-+1}\right)}{2} < m_- \text{ and } \bar{h}_- < 2\nu+1, \\ \bar{h}_-, & \text{otherwise;} \end{cases} \tag{3.20}$$

and

$$h_+ := \begin{cases} \bar{h}_+ - 1, & \text{if } \dfrac{\left(v_{\bar{h}_+} + v_{\bar{h}_+-1}\right)}{2} > m_+ \text{ and } \bar{h}_+ > 1, \\ \bar{h}_+, & \text{otherwise.} \end{cases} \tag{3.21}$$

In this way, the interval $I_{m,\sigma} := [v_{h_-}, v_{h_+}]$ has node endings that are the "half-nearest" ones, respectively, to the values $m_\pm$.

In this second case ψ_0 becomes, and this rule will be addressed to as the "OR" rule,

$$\psi_0^{h,i,n}(\ell) = \begin{cases} \left(\Delta_h(h_+ - h_- + 1)\right)^{-1}, & \text{if } h_- \leq h \leq h_+, \\ 0, & \text{otherwise.} \end{cases} \tag{3.22}$$

4. SIMULATIONS

Simulations have been performed to analyse the time evolution, and asymptotic behaviour, of a given initial distribution function. The analysis has been developed by varying not only some of the control parameters, but also those that assign initial conditions. In all cases, the qualitative shape of the initial condition distribution function has been maintained one and the same, namely the normal distribution function given by equation (2.7).

Different initial conditions have been realized by using different values for m_0 and σ_0, whereas the support $[-u_0, u_0]$ has always been chosen wide enough to appreciably include the complete normal distribution.

The total initial population N_0, that renormalizes the distribution function f, has been computed by means of the discretized version g^n of the function g_0 of equation (2.7) as follows:

$$N_0 = \sum_{n=1}^{2\nu+1} c\, g^n \Delta_n, \qquad \text{where } g^n := g_0(u = u_n), \tag{4.1}$$

and c is a scale constant to be conveniently set. In fact, it may be argued that c represents a further control parameter, to be compared with the time step intervals Δt_k of equation (3.7). In the following simulations, time steps have been chosen of the order of 10^{-2} (in particular: $\Delta t_k = 0.001$ for $0 \leq t_k \leq 0.2$ and $\Delta t_k = 0.01$ for $t_k > 0.2$); and the value $c = 50$ has been adopted when $m_0 = 0$ since it proved not to give rise to inconvenient oscillations. Moreover, the constants α and β of equation (2.18) have been fixed to $\alpha = 0.50$ and $\beta = 0.25$.

Experiment n.1

The first experiment of those cited in Section 2 is now discussed, and in particular for symmetric initial conditions: $m_0 = 0$. On the other hand, several of the considerations that may be done in this case hold for the others as well.

The main control parameter of this experiment is the occurrence probability q introduced in Section 2. On the contrary, the system shows no appreciable sensitivity to other parameters such as the initial condition variance σ_0, that has been fixed to a reference value of $\sigma_0 = 30$, and only a reduced sensitivity to the variance $\hat{\sigma}$ of the transition probability ψ, and even to which is the adopted one among the transition probabilities listed in Section 2.

Depending on the values of q, the system shows evolutions and, in particular, time asymptotic distribution f_∞, which may be grouped into three different kind of behaviours:

(1) localized forms,
(2) semi-localized forms, and
(3) dispersed forms.

They are characterized by the following facts.

(1) *Localized Forms*. In the localized forms, the distributions $f_k(u) := f(t = t_k, u)$ not only admit compact supports S_k at each $t = t_k$, $k = 0, 1, 2, \ldots$; yet, besides, nearly the entire initial population (i.e., a percentage greater than 99.6%) is localized on conveniently small intervals $L_k \subseteq S_k$ of the social state space. Here, the word "support" is meant to denote the set $S_k := \{u \mid f_k(u) \geq 10^{-8}\}$, and "compact" is to say: definitely smaller than (and properly contained in) $[A^*, B^*]$.

In other words, the whole population is gathered at each time within a small interval of social states.

In addition, if the conditions are generic, after a short transient of time past the initial condition all the intervals $L_{k \to \infty}$, assume one and the same finite length L, which increases directly with $\hat{\sigma}$ and inversely with q. Finally, when $m_0 = 0$, all the intervals L_k are centered around the origin.

An estimate of the length L of intervals L_∞ has been done as follows. If a threshold of $r = 0.01$ is adopted as an indicative value for the distribution function f_k, and L_∞ is identified with the set $\{u \mid f_\infty(u) \geq r\}$, then an estimate of L can be given by

$$L \sim 10\,\hat{\sigma}^{\gamma} q^{-2}, \qquad \text{where } \gamma := \begin{cases} 0.4, & \text{if } \psi = \psi_3, \\ 0.3, & \text{if } \psi = \psi_0, \end{cases} \tag{4.2}$$

as is briefly summarized by the experimental graph in Figure 1, where the technical values $\nu = 80$ and $\lambda = 8$ have been used, and where the barred ψ refer to the "AND" rule (3.19), and the unbarred ones to the "OR" rule (3.22).

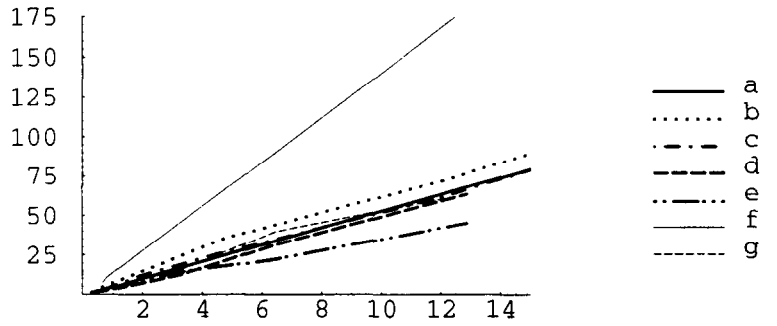

Figure 1. $q^2 L/2$ vs. $\hat{\sigma}^{\gamma}$. (a) $(\psi; q) = (\psi_3, \bar{\psi}_3; 0.8)$. (b) $(\psi; q) = (\psi_3, \bar{\psi}_3; 0.6)$. (c) $(\psi; q) = (\psi_3, \bar{\psi}_3; 0.7)$. (d) $(\psi; q) = (\psi_0; 0.8)$. (e) $(\psi; q) = (\psi_0; 0.6)$. (f) $(\psi; q) = (\bar{\psi}_0; 0.6)$. (g) $(\psi; q) = (\bar{\psi}_0; 0.8)$.

For small times the shape of the distribution functions obviously depends upon the choice $\psi_0, \ldots, \psi_3$, the mesh function ξ, and the value $\lambda := \log_{10} B^*$. Conversely, and if the conditions are far from a bifurcation region, the time asymptotic distribution f_∞ of the localized forms is stable and fairly independent of the mesh features.

Although this overall behaviour is shared by the time-asymptotic distributions f_∞ generated by $\psi_0, \ldots, \psi_3$, all the same some minor differences may be focused, that become more and more apparent the bigger is $\hat{\sigma}$. In particular, ψ_0 produces a higher and sharper tent-like figure, whereas ψ_3 yields a convex, flat, and smooth bump as it may be seen in Figure 2 that shows two f_∞ distributions, respectively, produced by ψ_0 (on the left-hand side) and by ψ_3 (on the right-hand side) starting from identical initial conditions (technical values are: $\nu = 80$, $\lambda = 8$, $\hat{\sigma} = 50$, $q = 0.8$).

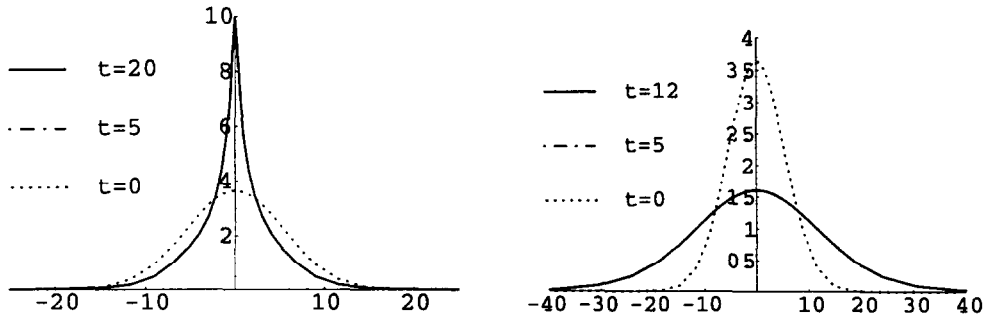

Figure 2. f vs. u; $\psi = \psi_0$ and $\psi = \psi_3$.

(2) *Semi-Localized Forms.* In the semilocalized forms, the distribution functions values generally decrease as k grows, in that the supports S_k become large although remaining definitely smaller than $[A^*, B^*]$. However, small intervals of social states may still be found that sustain

an appreciable percentage of the total population, and wherein the distribution function values are sufficiently high.

For times sufficiently great, the shape of the distributions may be loosely summarized as that of a horizontally drawn, upward aiming curly bracket, whose central small peak is placed at the origin, and whose big wings are stretched towards infinity. The wings profile generally decreases as the time flows, until a stable distribution f_∞ is reached such that the height of the two outer sides is much lower than that of the central bump. The central peak height may either only decrease with the time, or first decrease and then increase until it stabilizes to draw f_∞.

Although its shape depends upon the choice of ψ, the small central bump is anyway big enough to sustain a population N_r which is definitely greater than zero. If N_r is valued by

$$N_r = \sum_{n=1}^{2\nu+1} f_\infty^{n,r}\,\Delta_n, \qquad \text{where } f_\infty^{n,r} := \begin{cases} f_\infty^n, & \text{if } f_\infty^n \geq r := 0.01, \\ 0, & \text{otherwise,} \end{cases} \tag{4.3}$$

then the ratio $c_r := N_r/N_0$ is almost a constant

$$N_r \sim 0.02\,N_0, \tag{4.4}$$

in the sense that it is roughly independent of the mesh features, on the initial conditions' variance σ_0, on the transition variance $\hat{\sigma}$, and even on the choice of ψ. In the details, instead, the ratio c_r suffers not only of the drastic definition of N_r, but it also depends on the mesh. For instance, when different functions ξ are used, c_r varies from 0.1 to 0.02; or, in some cases when $\nu = 40$ is used instead of $\nu = 80$, it may become 0.04 instead of 0.02; and it slightly grows, directly with q and λ, inversely with $\hat{\sigma}$ and ν.

Concerning the differences between the time asymptotic distributions f_∞ generated by ψ_0 and those by ψ_3, the same may be said in the semilocalized as in the localized one; namely, they produce qualitatively similar dynamics. The details of the asymptotic distributions obviously depend on which is the adopted ψ. Yet, at generic conditions, differences are not so notable, and summarizable as above: ψ_0 produces a sharper tent-like figure, and ψ_3 a convex smooth bump. Only in some instances will ψ_0 yield a somewhat more uncertain dynamics, in that it shows to be more sensible than ψ_3 to variations of the other parameters, and ready to abandon standard behaviours in favour of nonstandard ones.

Figure 3 shows in bold lines the f_∞ functions produced by ψ_0 and ψ_3 in a semilocalized case (technical values are: $\nu = 80$, $\lambda = 8$, $\hat{\sigma} = 5$, $q = 0.5$).

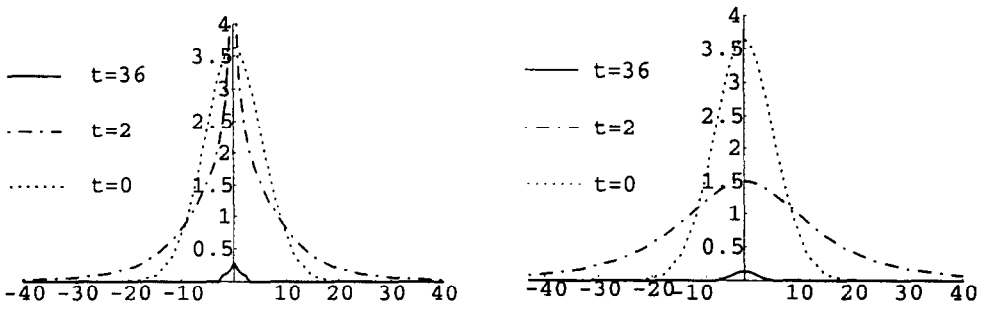

Figure 3. f vs. u; $\psi = \psi_0$ and $\psi = \psi_3$.

(3) *Dispersed Forms.* The case of dispersed distribution is self-explaining: nowhere is the value of the f_∞ distribution function greater than 0.01. Hence, now, one has $N_r = 0.0$ although here, as well as in both the preceding cases, the total integral $\sum_{n=1}^{2\nu+1} f_k^n\,\Delta_n$ (see equation (3.13)) of the distribution functions $\{f_k^n\}_{n=1,\ldots,2\nu+1}$ equals N_0 for each k. This third behaviour is observed, for

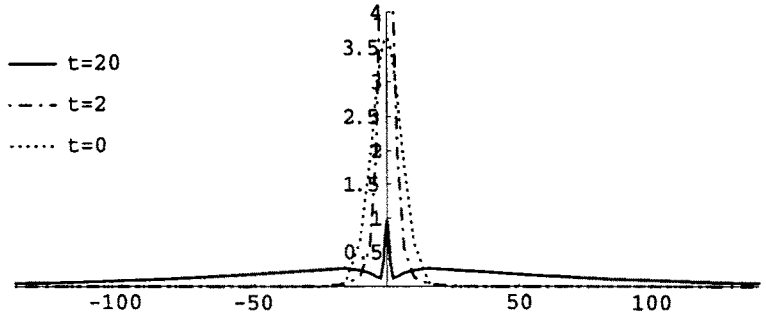

Figure 4. f vs. u; $\nu = 40$; $\lambda = 7$; $\hat{\sigma} = 0.5$; $q = 0.6$; $\psi = \bar{\psi}_3$.

instance, when $q = 0.0$ or when numeric or structural instabilities happen that brake the natural evolutions that give rise to either of the above discussed forms.

A hybrid form has also been observed, possessing a shape as in Case 2, but with the outer edges that maintain an appreciable part of the whole population, typically of the order of $0.5\,N_0$, and that show to be quite stable. These forms preferably appear when the node density is big ($\nu/\lambda \geq 10$) or in the very neighbourhood of a bifurcation.

As well it has been observed, although in very few cases, that a lower density of nodes may even act in favour, instead of contrasting, the localized form. It is sufficient, though, to operate small variations on the system conditions, such as replace ψ with $\bar{\psi}$, to break the numerical equilibrium and correctly remain into Case 2.

The following graphs summarize how the time asymptotic distribution functions f_∞ for Experiment n.1 vary on variations of the interaction probability variance $\hat{\sigma}$. Specifically, Figures 5 and 6 show the *semilocalized* asymptotic distributions, respectively, produced by $\psi = \psi_0$ and $\psi = \psi_3$. Figures 7 and 8 show the same graphs in the *localized* case. Initial conditions are identical for all of them. The graphs marked with a–e correspond to f_∞ distributions, respectively, produced by $\hat{\sigma} = 5 \times 10^h$ for $h = -1, 0, 1, 2, 3$. The graphs marked with f correspond to the initial conditions (technical values are: $\nu = 80$, $\lambda = 8$).

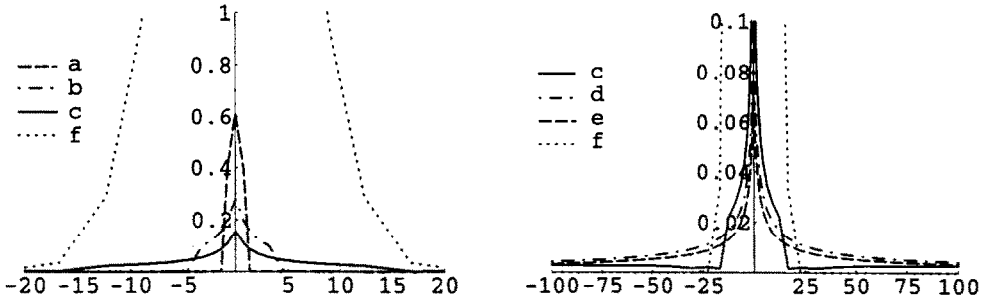

Figure 5. f_∞ vs. u; $\psi = \psi_0$; $q = 0.5$.

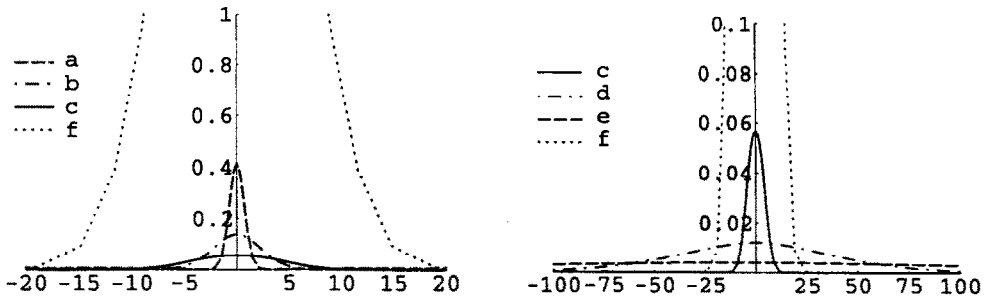

Figure 6. f_∞ vs. u; $\psi = \psi_3$; $q = 0.5$.

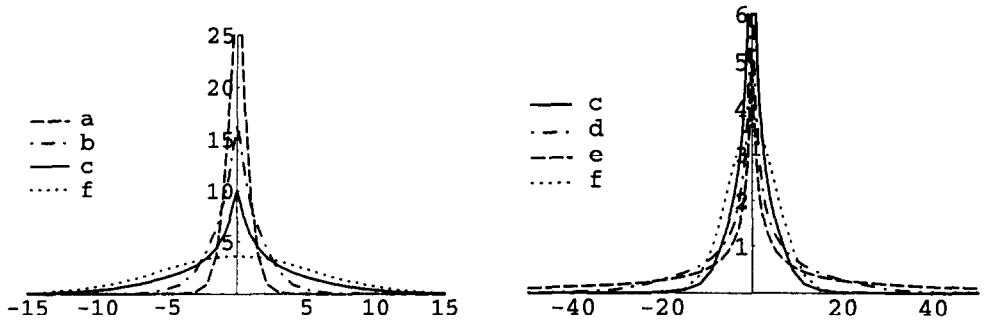

Figure 7. f_∞ vs. u; $\psi = \psi_0$; $q = 0.8$.

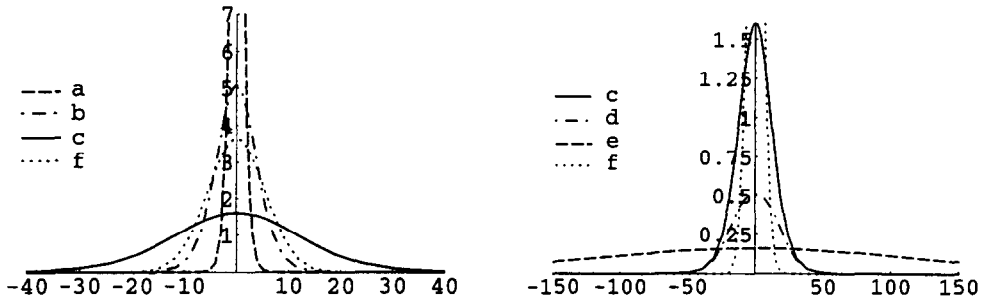

Figure 8. f_∞ vs. u; $\psi = \psi_3$; $q = 0.8$.

From the above figures, it is apparent that in this first experiment the parameter q is of primary importance in analysing which are the *a priori* conditions that yield Case 1, Case 2, or Case 3. Actually, when q ranges from 0 to 1, an abrupt change in the general behaviour of the system dynamics occurs, which shows features typical of a structural instability point; hence, in what follows, it will be addressed to as a bifurcation. In its neighbourhood, the dynamics not only shows a deeper dependence on the other control parameters such as the value $\hat{\sigma}$ of the transition variance, and on the choice of the adopted transition function ψ, but also on the technical characteristics, in the sense that if all the other parameters are assigned then a certain finite interval of values may be found such that, if q is fixed inside it, then the dynamics may still assume different forms depending on the choice of ξ, ν, λ. Figures 9a and 9b show two time evolutions that correspond to identical initial and structural conditions except the values of q. It may be noticed that small differences ($\sim 0.3\%$) on the values of q produce totally different dynamics and justify the name of bifurcation (technical values are: $\nu = 80$, $\lambda = 8$, $\hat{\sigma} = 5.0$, $\psi = \bar{\psi}_3$).

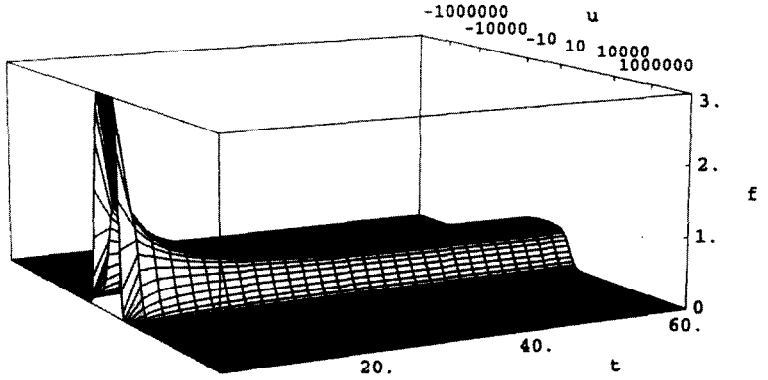

(a) f vs. (u, t); $q = 0.558$.

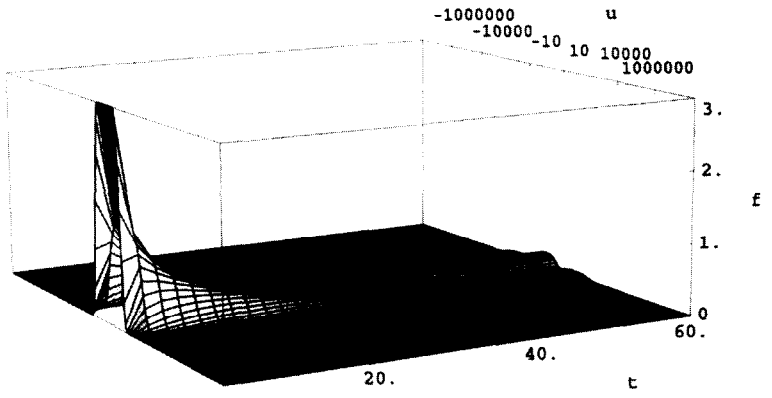

(b) f vs. (u, t); $q = 0.555$.

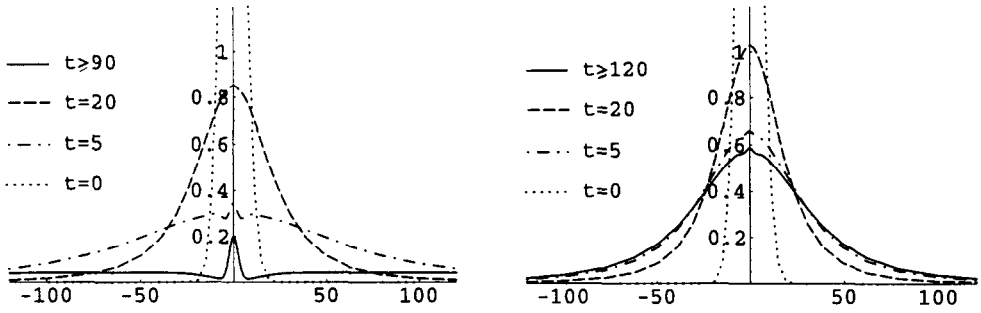

(c) f_∞ vs. u; $q = 0.558$ and $q = 0.555$.

Figure 9.

Quantitatively, the differences between the f_∞ functions in Figures 9a and 9b may be better appreciated in Figure 9c.

A more detailed analysis about the bifurcation region is difficult. What may safely be said is that values of q inside the interval $(0.0, 0.5)$ seemingly forbid the localized form to happen, whereas values of q in $(0.7, 1.0)$ easily allow us to sustain the whole population in a small interval. Values of q in each of these ranges yield evolutions which share the same qualitative behaviour, and this happens almost independently of the choices of $\hat{\sigma}$, σ_0, ξ, ν, λ, and even of ψ. Thus, structural instabilities are to be expected for q in the interval $(0.5, 0.7)$.

On the other hand, some side-factors make it difficult to establish a closer estimate of the bifurcation values. For instance, in the bifurcation region the dynamics may occasionally be influenced by the choice of the grid point function ξ, or the number of nodes ν, or the parameter λ. As well, in contrast with what happens at generic conditions, and in addition to the usual differences that are seen between the asymptotic distributions f_∞, in the neighbourhood of a bifurcation, discrepancies may be found due to which one is adopted ψ. In particular, the AND rule of Section 2 may create instabilities and hybrid cases in the dynamics near a bifurcation, especially if ψ_0 is used rather than ψ_3. Indeed, the AND rule may broaden the shape of the distributions (compared with those produced by the OR rule) to such an extent that the eventual distribution in the neighbourhood of a bifurcation may assume a hybrid form, or even suffer of poorness of nodes and be erroneously attributed to Case 2. Localized form distributions that are sensibly larger (and lower) than those allowed by equation (4.2) either prelude to a bifurcation, or produce some only seemingly stable distribution "f_∞" which in the long run proves to be unstable.

In conclusion, and apart from nongeneric conditions, the asymptotic distribution of this first experiment exists stable, as shown in Figures 5–8, and proves to be fairly independent of the values

(ν, λ) provided the ratio ν/λ is sufficiently great and the mean value of the initial distribution function is equal to zero.

At present, the same cannot be said about values of m_0 different from zero. Not only drastically different behaviours have been observed depending on the choice of ψ in the set $\{\psi_0, \bar{\psi}_0, \psi_3, \bar{\psi}_3\}$, but also an occasional dependence of the dynamics has been found upon the other controls, even the technical ones. Due to the relevant number of parameters, some more investigations are needed to sketch the complete picture.

As already mentioned, the generalities pointed out for Experiment n.1 hold true for the other two as well. Hence, and still in the m_0 case, a very brief report about these is here sufficient.

Experiment n.2

In this second case, the real constant c_e of equation (2.23) plays the role of interest. Indeed, parameter c_e assigns the shape and extension of the interaction, which is already very well localized due to the second power of the difference $(v - w)$; see equation (2.23). The larger c_e is, the more localized the interactions become.

As c_e varies, the system either shows a behaviour as in Case 1, or as in Case 3. The dynamics, instead, does not critically depend on the other structural parameters. Simulations have been accomplished for values of $\hat{\sigma}$ in the range $[0.5, 5000]$ and of c_e in the range $[10^{-1}, 10^{-11}]$, together with ψ_0 and ψ_3, and a neat bifurcation may be observed in the region $c_e \in (10^{-8}, 10^{-9})$, which do not appear to depend on $\hat{\sigma}$ or on the choice of the function ψ.

For $c_e \geq 10^{-8}$, no initial or structural condition has been found that allows the system to remain in the localized form of Case 1, and it eventually collapses into the dispersed Case 3.

For $c_e \leq 10^{-9}$, all the examined conditions maintain the localization of Case 1, and this happens independently of the mesh characteristics.

With some more detail, the system shows the following behaviour. At quite short times after the initial conditions $t = 0$, the system assumes a localized shape, in fact appreciably the same localized form it would have acquired under the same conditions in Experiment n.1 for q sufficiently great. Then, as the time grows, the probability distribution almost does not change at all. Subsequently, two different behaviours are observed. If $c_e \leq 10^{-9}$, the probability distribution function maintains its localized form asymptotically in time. Conversely, if $c_e \geq 10^{-8}$, after a certain period T of time, and almost abruptly, the whole distribution collapses to values less than 10^{-2} on the whole real axis. This Case 3 distribution function frequently shows maxima values around infinity, and it is the one that stably survives. The time T strongly depends on $\hat{\sigma}$ and c_e. Concisely, it may be said that T increases directly with $\hat{\sigma}$ and ν, and inversely with c_e and λ.

Just for the sake of completeness, it may be mentioned that the bifurcation interval for c_e may slightly depend on the adopted mesh generator ξ.

Experiment n.3

The structural parameter of this last case, in addition to the transition variance $\hat{\sigma}$, is the radius c_d of the interaction rule; see equation (2.24). Under the qualitative respects, in this experiment the system behaves exactly like in the previous one. As well, the parameter c_d is strong enough to effectively drive the system either to Case 1 or to Case 3; and, as well, bifurcation intervals for c_d may be found such that for lower values of c_d the system collapses after a transient and possibly long time T, whereas for higher values of c_d a localized form is stably attained. On the other hand, this experiment differs from the previous one in that the bifurcation intervals of the parameter c_d depend on the values of $\hat{\sigma}$, as is here briefly summarized.

Moreover, the above intervals may also depend on the node number, in that it may happen that the $\nu = 40$ case localizes whereas $\nu = 80$ collapses. However, this has been observed only in the bifurcation neighbourhoods.

Table 1. Bifurcation intervals for the parameter c_d.

	$\hat{\sigma} = 0.5$	$\hat{\sigma} = 5$	$\hat{\sigma} = 50$	$\hat{\sigma} = 500$	$\hat{\sigma} = 5000$
$\psi = \psi_0$	(100, 150)	(150, 200)	(150, 200)	(300, 350)	(1000, 1050)
$\psi = \psi_3$	(150, 200)	(150, 200)	(350, 400)	(1000, 1050)	(3350, 3400)

5. CONCLUSIONS

The last section contains a very brief discussion on the models described above.

Under the mathematical respects, none of them shows critical instabilities, with the exception of the conditions that characterize a bifurcation as those mentioned above. Under the numerical respects, the adopted discretization and numerical integration seem to be satisfying and appropriate to solve the problem for generic values of the controls and symmetric initial conditions. On the other hand, in the neighbourhood of a bifurcation, the system becomes so sensitive to each of the control parameters that any change of the conditions results in an *a priori* unpredictable, and sometimes *a posteriori* indecipherable, dynamics. All the same, when the whole structural picture is observed, the bifurcation may be fairly localized. Concerning the choice of the transition probability functions, the most stable and reliable appears to be $\psi = \psi_3$, namely the normal distribution together with the strict OR rule of the nearest node. Moreover, the function ψ_3 behaves as the most representative of those considered, in that the others give rise to dynamics that may be seen as a simple variation of the former one.

From the point of view of the physical interpretation, it may be said that even if the model is exceedingly simplified, all the same it does confirm everyday life expectations. Indeed, if the social rules are protective, the competition reduced, and the initial distribution balanced, then the model predicts that all the individuals eventually attain a comparable amount of wealth. Conversely, in a competitive society, the wealth distribution spreads more and more, and huge differences of social classes are allowed. In this case, only a small percentage of the population remains identifiable with a social status that is centered at the separation point between poverty and richness. Both these opposite behaviours are possibly tuned by minor details, yet they are stable and reproducible.

On the other hand, we feel that the times are not yet ready to develop a conclusive discussion in the cases that arise from an unbalanced initial distribution. Indeed, the question is still open concerning the dynamics starting from initial mean values away from the origin. Existing numerical results on this matter deserve some more investigation, both under the numerical and theoretical aspects.

REFERENCES

1. E. Jager and L. Segel, On the distribution of dominance in a population of interacting anonymous organisms, *SIAM J. Appl. Math.* **52**, 1442–1468, (1992).
2. N. Bellomo and M. Lo Schiavo, From the Boltzmann equation to generalized kinetic models in applied sciences, *Mathl. Comput. Modelling* **26** (7), 43–76, (1997).
3. N. Bellomo and M. Lo Schiavo, *Lecture Notes on the Mathematical Theory of Generalized Boltzmann Models*, World Scientific, Singapore, (1999).
4. N. Bellomo and E. De Angelis, Strategies of applied mathematics towards an immuno mathematical theory on tumors and immune system interactions, *Math. Models Meth. Appl. Sci.* **8**, 1403–1429, (1998).
5. E. De Angelis and L. Mesin, On the kinetic (cellular) theory. Conceptual frameworks on modelling the immune response, *Math. Models Meth. Appl. Sci.* **11**, (2001).
6. M. Lo Schiavo, A personalized kinetic model of traffic flow, *Traffic Flow—Modelling and Simulation*, Special Issue of *Mathl. Comput. Modelling*, (Edited by N. Bellomo) **35** (5/6), 607–622, (2001).
7. L. Arlotti, N. Bellomo and M. Lachowicz, Kinetic equations modelling populations dynamics, *Transp. Theory Statist. Phys.* **29**, 125–139, (2000).
8. L. Arlotti, N. Bellomo and K. Latrach, From the Jager and Segel model to kinetic population dynamics nonlinear evolution problems and applications, *Mathl. Comput. Modelling* **30** (1/2), 15–40, (1999).
9. B. Firmani, L. Guerri and L. Preziosi, Tumor/immune system competition with medically induced activation/disactivation, *Math. Mod. Meth. in Appl. Sci.* **9** (4), 491–512, (1999).

10. A. Samarskii, Monotone difference schemes for equations with mixed derivatives, *Computers Math. Applic.* **44** (3/4), 501–510, (2002).
11. P. Auger, R. Bravo de la Parra and E. Sanchez, Behavioural dynamics of two interacting hawk-dove populations, *Math. Models Meth. Appl. Sci.* **11** (4), (2001).